Molecular Crystals and Liquid Crystals

Publication details, including instructions for authors and subscription information:
http://www.tandfonline.com/loi/gmcl20

Viscoelastic Flows of Cholesteric Liquid Crystals

E. Orlandini [a] , D. Marenduzzo [b] & J. M. Yeomans [c]

[a] Dipartimento di Fisica, Universita' di Padova, and Sezione INFN, Via Marzolo, Padova, Italy

[b] SUPA, School of Physics, University of Edinburgh, Mayfield Road, Edinburgh, UK

[c] The Rudolf Peierls Centre for Theoretical Physics, Oxford, UK

Version of record first published: 22 Sep 2010

To cite this article: E. Orlandini, D. Marenduzzo & J. M. Yeomans (2007): Viscoelastic Flows of Cholesteric Liquid Crystals, Molecular Crystals and Liquid Crystals, 465:1, 1-14

To link to this article: http://dx.doi.org/10.1080/15421400701205347

Mol. Cryst. Liq. Cryst., Vol. 465, pp. 1–14, 2007

ISSN: 1542-1406 print/1563-5287 online
DOI: 10.1080/15421400701205347

Taylor & Francis
Taylor & Francis Group

Viscoelastic Flows of Cholesteric Liquid Crystals

E. Orlandini
Dipartimento di Fisica, Universita' di Padova, and Sezione INFN, Via Marzolo, Padova, Italy

D. Marenduzzo
SUPA, School of Physics, University of Edinburgh, Mayfield Road, Edinburgh, UK

J. M. Yeomans
The Rudolf Peierls Centre for Theoretical Physics, Oxford, UK

We numerically solve the hydrodynamic equations of motion for a cholesteric liquid crystal under an imposed Poiseuille flow, by means of lattice Boltzmann simulations. The elasticity of the cholesteric helix couples to the external flow to give rise to a highly viscoelastic flow. This is a technically difficult problem for standard flow solvers due to its fully two-dimensional nature. We consider a helix with axis parallel to the boundaries, and at the same time to either the primary flow or the vorticity direction (we identify these two flow modes as permeation and vorticity mode respectively). We quantify the large difference found in the steady state director and velocity profiles, and in the apparent viscosities obtained in the two cases.

Keywords: cholesterics; lattice Boltzmann method; rheology

INTRODUCTION

Liquid crystals are fluids, typically comprising long thin molecules, where subtle energy–entropy balances can cause the molecules to align to form a variety of ordered states [1,2]. In nematic liquid crystals the molecules tend to align parallel giving a state with long-range orientational order. This is usefully described by the director field $\vec{n}$, the axis along which molecules are preferentially aligned. In a cholesteric or

This work was supported by EPSRC grant no. GR/R83712/01 and SUPA.
Address correspondence to E. Orlandini, Dipartimento di Fisica, Universita' di Padova, and Sezione INFN, Via Marzolo 8, Padova 35131, Italy. E-mail: orlandini@pd.infn.it

chiral nematic liquid crystal $\vec{n}$ has a natural twist deformation. Examples of cholesteric liquid crystals are DNA molecules in solution, colloidal suspensions of bacteriophages [3], and solutions of nematic mixtures such as E7 with chiral dopants which are widely used in display devices [4].

Liquid crystals exhibit both an elastic and a viscous response to an external stress [1,2]. Coupling between the director and the velocity fields–known as back-flow–leads to strongly non-Newtonian flow behaviour.

The non-Newtonian character of liquid crystal flow is apparent in cholesterics rheology. One striking example is *permeation*. When a cholesteric liquid crystal is subjected to an imposed flow in the direction that its helix axis attains in the cholesteric phase, its viscosity can increase enormously (by a factor $\sim 10^5$) with respect to that of the same material in the isotropic phase [5–13]. An explanation of permeation was given by Helfrich [5]. If the director orientation is fixed in space, due for example to anchoring effects at the wall, any flow along the helix must be linked to a rotation of the molecules. This leads to an energy dissipation far larger than that due to the usual molecular friction and hence a much enhanced viscosity.

The possibility of permeative flows and of other complex back-flow effects has slowed down quantitative theoretical and simulation work on the rheology of cholesterics, which presently lies on significantly less solid grounds than its overall well-established and understood nematic counterpart. Indeed the intricacy of the hydrodynamic equations of motion, which are highly non-linear and require an accurate resolution of length scales smaller than or comparable to the helical pitch, have narrowed the scope of most theoretical analyses to largely simplified geometries and weak flows. These have nonetheless highlighted the richness of the rheological properties of these materials.

Most of the previous literature in the field consists in semi-analytical approximate treatments of permeation flow [1,5,14–16,20,21] and of flow with the helical axis along the velocity gradient direction [17], although some studies of other geometries exist [18,19]. These semi-analytical calculations are often highly simplified, e.g., permeation theories typically assume (i) very weak forcing (so that the director field is only perturbatively deformed by the flow), (ii) no secondary flow, and (iii) a constant order parameter throughout the sample. In geometries different from the one leading to permeation, (i) and (ii) have sometimes been relaxed, while (iii) is almost invariably employed. These simplifications limit progress: for example within these treatments there is no way of predicting how the director field is deformed by a strong permeative flow, or of quantitatively predicting viscosity versus shear curves for different flows and geometries.

Recently, in Refs. [22–24] we have proposed a lattice Boltzmann algorithm which solves the Beris-Edwards equations of motion for the hydrodynamics of liquid crystals. We have shown that this method is robust and numerically remarkably stable, so that it allows a quantitative study of the rheology of cholesterics, which nicely complements the semi-analytical approaches previously proposed in the literature, as it makes it possible to answer questions which cannot be answered analytically. For instance, we now know that a strong Poiseuille or shear flow in the permeation mode can stabilise substantially distorted director patterns [25,26], in which the cholesteric layers can either bend into chevrons or reorganise into doubly twisted texture. We have also been able to map out [26,27] viscosity versus forcing curves which prove (i) that there is strong shear thinning if the director field is anchored at the boundary (ie if fixed boundary conditions are used), and (ii) that the shape of these curves is extremely sensitive to the type of boundary conditions employed. Further studies have highlighted that this lattice Boltzmann algorithm can even allow a controlled study of the static and rheological properties of blue phases [28, 29], which are a series of phases typically encountered in the vicinity of the isotropic-to-cholesteric transition, consisting of periodic networks of disclination lines [30]. Given the importance of cholesterics in optical devices and biological DNA solutions and the ubiquity of permeative flow in the theory of layered liquid crystals [31], it is extremely important to have and further develop a robust numerical framework within which to systematically analyse the flow properties of cholesterics. Moreover the advent of micro-channel technology means that quantitive experiments to test theoretical predictions are likely to be or soon become feasible.

In this work we present new results obtained by applying our lattice Boltzmann algorithm to study Poiseuille flow in a flow-aligning cholesteric liquid crystal with its helix lying along the vorticity direction (hereafter vorticity mode, i.e., along the direction of secondary flow), and compare the director and velocity profiles at steady state with those found with the helix along the *primary* flow direction (i.e., in the permeation mode). We find that in both cases the apparent viscosity of the liquid crystal decreases with increasing forcing, so that the material is shear thinning. However the magnitude of this shear thinning is vastly different and is much larger in the permeation mode. In both cases the external flow induces a twisting along the velocity gradient direction, which is enhanced by our choice of boundary conditions. Secondary flow is present in both the vorticity and the permeation mode, but while in the former case it is small with respect to the primary flow, in the latter it may be much larger.

The article is organized as follows. In section II, we review the hydrodynamic equations of motion for cholesterics which we set out to solve. In section III, we present results for Poiseuille flow in the vorticity and permeation mode. Finally, section IV contains our conclusions.

EQUATIONS OF MOTION

We consider the formulation of liquid crystal hydrodynamics given by Beris and Edwards[32,33], generalized for cholesteric liquid crystals.

The equations of motion are written in terms of a tensor order parameter $\mathbf{Q}$ which is related to the direction of individual molecules, $\hat{n}$, by $Q_{\alpha\beta} = \langle \hat{n}_\alpha \hat{n}_\beta - 1/3\,\delta_{\alpha\beta} \rangle$ where the angular brackets denote a coarse-grained average and the Greek indices label the Cartesian components of $\mathbf{Q}$. The tensor $\mathbf{Q}$ is traceless and symmetric. Its largest eigenvalue, $2/3\,q, 0 < q < 1$, describes the magnitude of the order.

The equilibrium properties of the liquid crystal are described by a Landau-de Gennes free energy density. This comprises a bulk term (summation over repeated indices is implied hereafter),

$$f_b = \frac{A_0}{2}\left(1 - \frac{\gamma}{3}\right)Q_{\alpha\beta}^2 - \frac{A_0\gamma}{3}Q_{\alpha\beta}Q_{\beta\gamma}Q_{\gamma\alpha} + \frac{A_0\gamma}{4}(Q_{\alpha\beta}^2)^2, \tag{1}$$

which describes a first-order transition from the isotropic to the chiral phase at $\gamma = 2.7$, together with a an elastic contribution which for cholesterics is [1]

$$f_d = \frac{K}{2}\left[(\partial_\beta Q_{\alpha\beta})^2 + \left(\epsilon_{\alpha\zeta\delta}\partial_\zeta Q_{\delta\beta} + \frac{4\pi}{p}Q_{\alpha\beta}\right)^2\right], \tag{2}$$

where K is an elastic constant and p is the helix pitch. The tensor $\epsilon_{\alpha\zeta\delta}$ is the Levi-Civita asymmetric third-rank tensor, A_0 is a constant and γ controls the magnitude of order. (it plays the role of an effective temperature or concentration according to whether the cholesteric liquid crystal is thermotropic or lyotropic). The anchoring of the director field on the boundary surfaces is ensured by adding a pinning term

$$f_S = \frac{1}{2}W_0(Q_{\alpha\beta} - Q_{\alpha\beta}^0)^2 \tag{3}$$

with $Q_{\alpha\beta}^0$ typically of the form

$$Q_{\alpha\beta}^0 = S_0(n_\alpha^0 n_\beta^0 - \delta_{\alpha\beta}/3). \tag{4}$$

The parameter W_0 controls the strength of the anchoring, while S_0 determines the magnitude of surface order. If the surface order is

equal to the bulk order (as is the case in the simulations reported here), S_0 should be taken equal to q.

The equation of motion for $\mathbf{Q}$ is [32]

$$(\partial_t + \vec{u}\cdot\nabla)\mathbf{Q} - \mathbf{S}(\mathbf{W},\mathbf{Q}) = \Gamma\mathbf{H} \tag{5}$$

where Γ is a collective rotational diffusion constant. The first term on the left-hand side of Eq. (5) is the material derivative describing the usual time dependence of a quantity advected by a fluid with velocity $\vec{u}$. This is generalized for rod-like molecules by a second term

$$\mathbf{S}(\mathbf{W},\mathbf{Q}) = (\xi\mathbf{D}+\mathbf{\Omega})(\mathbf{Q}+\mathbf{I}/3) + (\mathbf{Q}+\mathbf{I}/3)(\xi\mathbf{D}-\mathbf{\Omega}) - 2\xi(\mathbf{Q}+\mathbf{I}/3)\mathrm{Tr}(\mathbf{QW}) \tag{6}$$

where Tr denotes the tensorial trace, and $\mathbf{D} = (\mathbf{W}+\mathbf{W}^T)/2$ and $\mathbf{\Omega} = (\mathbf{W}-\mathbf{W}^T)/2$ are the symmetric part and the anti-symmetric part respectively of the velocity gradient tensor $W_{\alpha\beta} = \partial_\beta u_\alpha$. $\mathbf{S}(\mathbf{W},\ \mathbf{Q})$ appears in the equation of motion because the order parameter distribution can be both rotated and stretched by flow gradients. This is a consequence of the rodlike geometry of the LC molecules. The constant ξ depends on the molecular details of a given liquid crystal. The term on the right-hand side of Eq. (5) describes the relaxation of the order parameter towards the minimum of the free energy. The molecular field H which provides the driving motion is given by

$$\mathbf{H} = -\frac{\delta\mathcal{F}}{\delta\mathbf{Q}} + (\mathbf{I}/3)Tr\frac{\delta\mathcal{F}}{\delta\mathbf{Q}}. \tag{7}$$

The three-dimensional fluid velocity, $\vec{u}$, obeys the continuity equation

$$\partial_t\rho + \partial_\alpha(\rho u_\alpha) = 0 \tag{8}$$

and the Navier–Stokes equation,

$$\rho(\partial_t + u_\beta\partial_\beta)u_\alpha = \partial_\beta(\Pi_{\alpha\beta}) + \eta\partial_\beta(\partial_\alpha u_\beta + \partial_\beta u_\alpha + (1-3\partial_\rho P_0)\partial_\gamma u_\gamma\delta_{\alpha\beta}), \tag{9}$$

where ρ is the fluid density and η is an isotropic viscosity. The form of this equation is similar to that for a simple fluid. However, the details of the stress tensor, $\Pi_{\alpha\beta}$, reflect the additional complications of liquid crystals hydrodynamics. The pressure tensor is explicitly given by:

$$\begin{aligned}\Pi_{\alpha\beta} = {} & -P_0\delta_{\alpha\beta} + 2\xi\left(Q_{\alpha\beta}+\frac{1}{3}\delta_{\alpha\beta}\right)Q_{\gamma\epsilon}H_{\gamma\epsilon} - \xi H_{\alpha\gamma}\left(Q_{\gamma\beta}+\frac{1}{3}\delta_{\gamma\beta}\right) \\ & - \xi\left(Q_{\alpha\gamma}+\frac{1}{3}\delta_{\alpha\gamma}\right)H_{\gamma\beta} - \partial_\alpha Q_{\gamma\nu}\frac{\delta\mathcal{F}}{\delta\partial_\beta Q_{\gamma\nu}} + Q_{\alpha\gamma}H_{\gamma\beta} - H_{\alpha\gamma}Q_{\gamma\beta}.\end{aligned} \tag{10}$$

The background pressure P_0 is constant, in the simulations reported here, to a very good approximation ($\pm 1\%$). It should be noted that the order parameter field affects the dynamics of the flow field through the stress tensor (10), which appears in the Navier–Stokes Eq. (9) and depends both on Q and H. This back action of the order parameter field on the flow is usually referred to as back-flow.

To study these equations we use a lattice Boltzmann algorithm. Details and validation of using this method to solve the Beris-Edwards model were given in Refs. [22,23] for the two-dimensional case and in Ref. [24] for the three-dimensional one. In the present work we chose a slightly different prescription for the implementation of the lattice Boltzmann algorithm with respect to the one presented in Ref. [24]. Instead of using $\Pi_{\alpha\beta}$ to constrain the second moment of the velocity distribution functions as in Ref. [24], the derivative of the pressure tensor, $\partial_\beta \Pi_{\alpha\beta}$ is here directly entered as a body force. This scheme reduces spurious velocities down to machine precision in the case under consideration.

It is possible to write down a relation between the six viscosity coefficients $\alpha_1, \ldots, \alpha_6$ characterising nematodynamics within the Leslie-Ericksen model [1], and the parameters of the Beris-Edwards model. These are [22,32]

$$\begin{aligned}
\alpha_1 &= -\frac{2/3q^2(3+4q-4q^2)\xi^2}{\Gamma}, \\
\alpha_2 &= \frac{(-1/3q(2+q)\xi - q^2)}{\Gamma}, \\
\alpha_3 &= \frac{(-1/3q(2+q)\xi + q^2)}{\Gamma}, \\
\alpha_4 &= \frac{4/9(1-q)^2\xi^2}{\Gamma+\eta}, \\
\alpha_5 &= \frac{(1/3q(4-q)\xi^2 + 1/3q(2+q)\xi)}{\Gamma}, \\
\alpha_6 &= \frac{(1/3q(4-q)\xi^2 - 1/3q(2+q)\xi)}{\Gamma}.
\end{aligned} \tag{11}$$

Particularly relevant quantities are the rotational viscosity $\gamma_1 \equiv \alpha_3 - \alpha_2 = 2q^2/\Gamma$ and the ratio between α_3 and α_2. If $\alpha_3/\alpha_2 > 0$ the liquid crystal is flow aligning, otherwise it is flow tumbling. We will restrict ourselves to the former case for the simulations reported in this work.

RESULTS

We now discuss the results which we have obtained by applying our lattice Boltzmann flow solver to study Poiseuille flow in a slab of cholesteric liquid crystal sanwiched between two planes parallel to the xy plane, when the axis of the cholesteric helix lies along y. We consider two cases: (a) that of an induced flow along x (vorticity mode, i.e., the cholesteric helix then lies along the vorticity direction), and (b) that of a flow along y (i.e., the permeation mode). For simplicity we restrict ourselves to the case in which the director field at the boundaries is fixed to the zero flow configuration (fixed boundary conditions). This is quite a common choice in the literature on the rheology of cholesterics, which can be physically realised by impurities, pinning the helix at the boundaries [6–12]. For a systematic analysis of the effects of boundary conditions on rheological properties for Poiseuille and shear flow in the permeation and velocity gradient modes the reader is referred to [25,26,34,35]. The geometry of the initial condition and of the external flows we consider are shown in Figure 1. In the case of a Newtonian fluid, it is well known that the (Poiseuille) flow we have chosen leads to a quadratic primary velocity field (and no secondary flow).

We consider channel widths $L \sim 2\,\mu$m, and the elastic constant is 5 pN, which corresponds to the case of all three Frank elastic constants equal to 2.5 pN. The ratio between α_3 and α_2 is 0.08 while $\gamma_1 = 1$ Poise. We will henceforth use simulation units for space and time measurements. These can be mapped to physical units by noting that one space and time step correspond respectively to $0.022\,\mu$m and $0.667\,\mu$s respectively. In the following we will quantify the strength of the forcing via the value of the dimensionless parameter $\tilde{f} = \Delta p L^2/\eta c$, where Δp is the imposed pressure difference, η is the isotropic viscosity entering the Navier Stokes equations, and c is the sound velocity (see Refs. [22–24] for details on how to compute η and c in our lattice Boltzmann algorithm).

We first consider case (i), namely flow in the vorticity mode with fixed boundary conditions. We note that we are neglecting changes in the helical pitch due to the flow, which is legitimate provided that fixed boundary conditions are used. The pitch widens with flow before the helical structure is disrupted, in the treatment neglecting boundary effects proposed in Ref. [14].

Figure 2, column 1, shows the director (a) and velocity (b) profile for quite strong Poiseuille flow ($\tilde{f} = 1.83$). The cholesteric layers are bent by the perpendicular flow in an S-shaped pattern, so that there is a component of the director field along the flow direction.

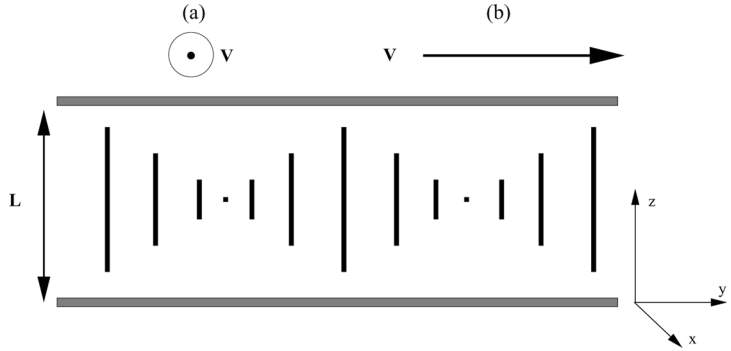

FIGURE 1 Geometries used for the simulation described in the text. The liquid crystal is sandwiched between two infinite plates, parallel to the xy plane, lying at $z = 0$ and $z = L$. The arrows in (a) and in (b) denote the directions of the primary flow induced by the imposed pressure difference in the vorticity and permeation mode respectively.

(The maximum value of the absolute value of the component of the director field along y is ~ 0.37.) The bending of the director field induces a flow-induced twist along the velocity gradient direction (i.e., the z direction), which couples to the original twist along the y direction to give regions of non-zero double twist. The velocity profile (Fig. 2b) shows that the flow is non-Newtonian, with a secondary flow along the helical direction which is antisymmetric with respect to the centre channel and which ultimately leads to the S-shaped of the director field deformation just described. However, the values of the pressure difference needed to significantly distort the director field are remarkably high, which signals that the fingerprint texture (the technical name for the structure depicted in Fig. 1) is very stable when it lies along the vorticity direction of the imposed flow.

A very different situation is encountered when the cholesteric helix is subjected to flow in the permeation mode (i.e., along the y axis, see Fig. 1b). In that case the structure is much less stable and more sensitive to the flow, as can be seen by comparing the director field deformation and velocity profiles in steady state in Figure 3 in the vorticity (Fig. 3, first column) and in the permeation (Fig. 3, second column) modes. The forcing is the same in both calculations ($\tilde{f} \sim 0.03$). The director develops a larger component along y in the permeation mode (Fig. 3, (2a), ~ 0.14 in absolute value as opposed to ~ 0.02 in the vorticity mode, Figure 3, (1a)). There is secondary flow in both cases but this is much larger in magnitude in the permeation mode

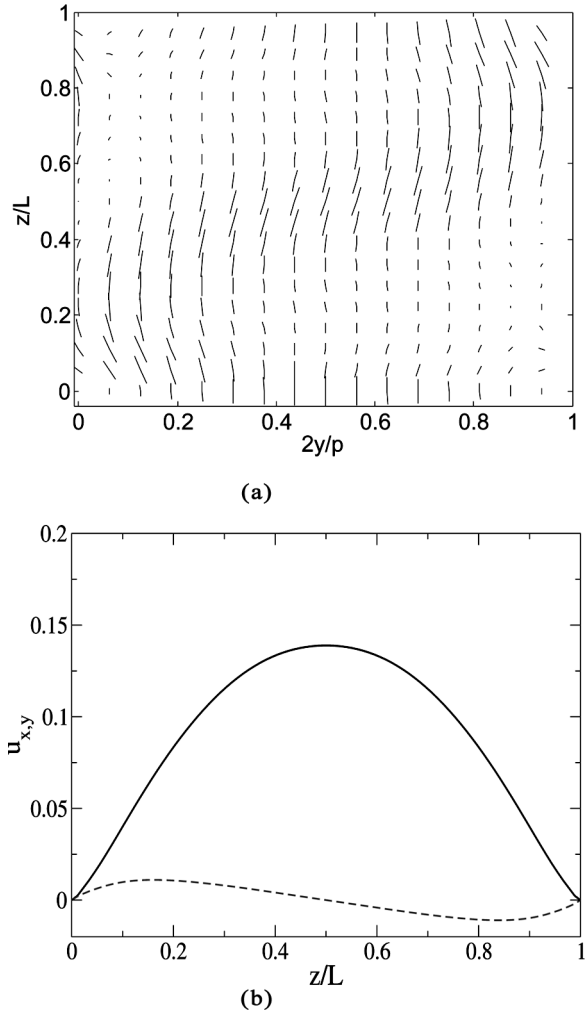

FIGURE 2 Plot of (a) director and (b) velocity profiles for a cholesteric under Poiseuille flow in the vorticity mode with $\tilde{f} = 1.83$.

(compare Fig. 3, (2b) with Fig. 3, (1b)). In the permeation mode the cholesteric layers are bent into a chevron like structure, and hardly move. The maximum velocity attained by the primary flow is ~ 50 times smaller than that of a corresponding isotropic fluid in the same geometry and subject to the same pressure difference (simulated by switching off backflow), in agreement with semi-analytic approaches on Poiseuille flow in the permeation mode [1,5].

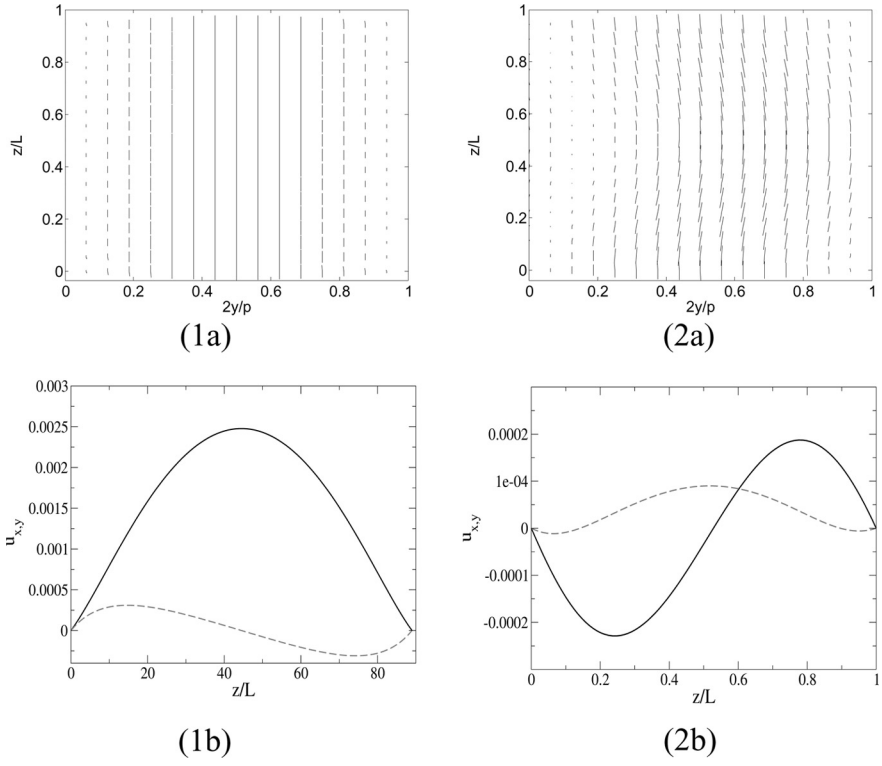

FIGURE 3 Plot of director and velocity profiles for a cholesteric under Poiseuille flow in the vorticity (respectively (1a) and (1b)) and permeation (respectively (2a) and (2b)) mode. These results were obtained with $\tilde{f} = 0.04$.

The origin of the chevron pattern in the permeation mode can be identified by considering Eq. (5), under the approximation that back-flow is neglected. Focussing on the center of the channel, S is zero, and the term $\vec{u} \cdot \vec{\nabla}\mathbf{Q}$ must be balanced by a drift of the layers, $\partial_t \mathbf{Q}$. That the term $\vec{u} \cdot \vec{\nabla}\mathbf{Q}$ may be non-zero is typical of the permeation mode, as the director field is not constant along the flow direction. However, due to the parabolic shape of the velocity field, these cannot cancel exactly and it is necessary to allow for a non-zero molecular field, resulting in the observed bending from the equilibrium configuration. The dominant elastic deformations associated with this steady state solution are splay-bend. The director field also develops a small component along the flow direction. This is caused by the shear forces contained in the tensor S, which is non-zero away from the centre of the channel and as is well known forces some flow-induced alignment

of the director field. In the vorticity mode a similar perturbation is still driven by u_y, which is however the *secondary* and not the *primary* flow in that geometry, and this explains why the helical structure is much more stable in the vorticity mode.

As the pressure difference is increased in the permeation mode, we find that the chevrons bend gradually until the pressure difference

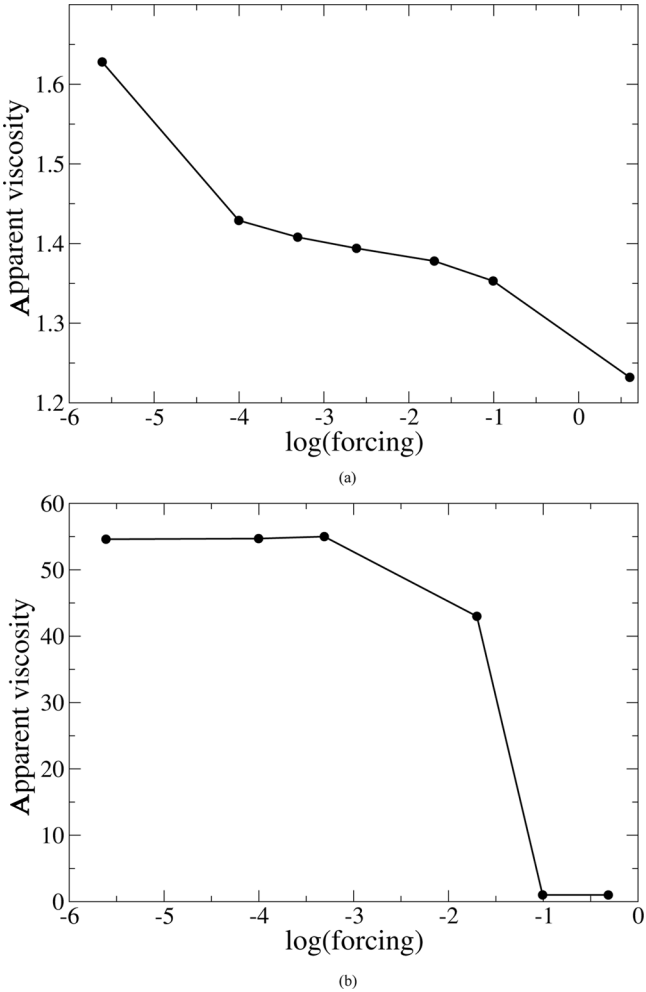

FIGURE 4 Apparent viscosity versus (logarithm of) dimensionless forcing for a cholesteric liquid crystal under Poiseuille flow in the (a) vorticity and (b) permeation mode.

reaches a threshold above which they no longer describe the steady state director profile of the system and are replaced by a doubly twisted texture, as previously reported for liquid crystals with different values of ξ (and hence α^3/α^2).

We now turn to the determination of the apparent viscosity of the cholesteric liquid crystal in the vorticity and permeation mode. In the geometry we consider the volumetric flow rate for a Newtonian fluid is

$$\frac{\Phi}{L_x} = \frac{\Delta p}{12\eta} L^3 \tag{12}$$

where L_x is the transverse direction (along x in Fig. 1). We can thus define an apparent viscosity η_{app}, by requiring Eq. (12) to still hold for a non-Newtonian fluid, but with η_{app} replacing η. We can also define a relative viscosity $\eta_{\text{rel}} = \eta_{\text{app}}/\eta$. This is plotted as a function of the dimensionless forcing in Figure 4 for both the permeation and the vorticity mode.

In the permeation mode (Fig. 4b) it can be seen that the apparent viscosity is, for small forcing, ~ 50 times larger than the one corresponding to a non-Newtonian fluid with the same parameters. This can be understood as a backflow effect: the flow bends the layers into chevrons, which as they try to straighten out induce a large backflow which works against the imposed pressure difference to give a very small net velocity. For stronger forcing there is shear thinning associated with the breaking of the helices and the viscosity becomes comparable to that of an isotropic fluid.

Figure 4a shows the corresponding viscosity versus forcing curve found in the vorticity mode. It can be seen that the liquid crystal flows much more easily, as the apparent viscosity is comparable to that of a corresponding Newtonian fluid this time. The cholesteric liquid crystal still shear thins, as found also in Ref. [19], but the extent of this shear thinning is greatly reduced with respect to the permeation mode.

CONCLUSIONS

In conclusion, we have presented lattice Boltzmann simulations to study Poiseuille flow in a cholesteric liquid crystal in the vorticity and permeation mode (i.e., with the cholesteric helix parallel to the boundary plates and an imposed flow respectively either perpendicular or parallel to this axis). There are some similarities in the two geometries, in that in both cases (i) the fluids shear thins upon increasing the pressure difference which drives the flow, and (ii) the director field develops a non-equilibrium flow-induced twist along

the velocity gradient direction (i.e., perpendicular to the direction of the original twist in the initial condition). However, there are remarkable differences, most notably in the value of the apparent viscosity which is more than an order of magnitude larger in the permeation mode due to the enhanced elastic stresses experienced by the system in this flow mode.

We note that the few theoretical and numerical studies of flow in cholesterics in the vorticity mode [18,19] considered a steady shear flow and neglected boundary effects (considered free boundary conditions and an effectively one-dimensional situation). Under those approximations it was found that a shear flow could either excite twist waves in which the director field was planar, i.e., there was no component along the shear flow, or induce a non-equilibrium phase transition to a nematic phase for strong enough shear. It is therefore not appropriate to directly compare those calculations with ours, which is fully two-dimensional, and considers Poiseuille flow with fixed boundary conditions. However our simulations suggest that if the director field is fixed to the boundary e.g., by some impurity or surface defect (as is typically assumed to be the case at least in the permeation mode) it is likely that a non-zero component of the director field along the flow will appear. In view of the small numbers of simulation papers on the vorticity flow mode in cholesterics, it seems interesting to generalise the present simulations to cover a steady shear flow and different boundary conditions as well. Experiments with flow in the vorticity mode seem to be now feasible, and by comparing them to quantitative predictions e.g. for viscosity versus shear curves obtained numerically from 3-dimensional lattice Boltzmann simulations it will be possible to enhance our understanding of cholesterics rheology. This appears to be a promising avenue for future research in the field in view of the fact that an imposed flow in the vorticity mode can be analysed numerically more straightforwardly than one in the permeation mode.

REFERENCES

[1] de Gennes, P. G. & Prost, J. (1993). *The Physics of Liquid Crystals, 2nd Ed.*, Clarendon Press: Oxford.
[2] Chandrasekhar, S. (1980). *Liquid Crystals*, Cambridge University Press: Cambridge.
[3] Grelet, E. & Fraden, S. (2003). *Phys. Rev. Lett.*, *90*, 198302.
[4] Raynes, E. P., Brown, C. V., & Stromer, J. F. (2003). *Appl. Phys. Lett.*, *82*, 13; Stromer, J. F., Marenduzzo, D., Brown, C. V., Yeomans, J. M., & Raynes, E. P. (2006). *J. Appl. Phys.*, *99*, 064911.
[5] (a) Helfrich, W. (1969). *Phys. Rev. Lett.*, *23*, 372.
(b) Lubensky, T. C. (1969). *Phys. Rev. A*, *6*, 452.

[6] Porter, R. S., Barrall, E. M., & Johnson, J. F. (1966). *J. Chem. Phys*., *45*, 1452.
[7] Scaramuzza, N., Simoni, F., Bartolino, R., & Durand, G. (1984). *Phys. Rev. Lett*., *53*, 2246.
[8] Hongladarom, K., Secakusuma, V., & Burghardt, W. R. (1994). *J. Rheol*., *38*, 1505.
[9] Scaramuzza, N., Carbone, V., & Barberi, R. (1991). *Mol. Cryst. Liq. Cryst*., *195*, *31*.
[10] Bhattacharya, S., Hong, C. E., & Letcher, S. V. (1978). *Phys. Rev. Lett*., *41*, 1736.
[11] Ramos, L., Zapotocky, M., Lubensky, T. C., & Weitz, D. A. (2002). *Phys. Rev. E*, *66*, 031711.
[12] Zapotocky, M., Ramos, L., Poulin, P., Lubensky, T. C., & Weitz, D. A. (1999). *Science*, *283*, 209.
[13] Negita, K. (1998). *Liq. Cryst*., *24*, 243.
[14] Rey, A. D. (2000). *J. Rheol*., *44*, 855.
[15] Rey, A. D. (2002). *Phys Rev. E*, *65*, 022701.
[16] Rey, A. D. (2002). *J. Rheol*., *46*, 225.
[17] Leslie, F. M. (1979). *Adv. Liq. Cryst*., *4*, 1.
[18] Derfel, G. (1983). *Mol. Cryst. Liq. Cryst*., *92*, *41*.
[19] Rey, A. D. (1996). *J. Non-Newtonian Fluid Mech*., *64*, 207.
[20] Prost, J., Pomeau, Y., & Guyon, E. (1991). *J. Phys. II*, *1*, 289.
[21] Cui, Z. L., Calderer, M. C., & Wang, Q. (2006). *Disc. Cont. Dyn. Syst. B*, *6*, 291.
[22] Denniston, C., Orlandini, E., & Yeomans, J. M. (2000). *Europhys. Lett*., *52*, 481.
[23] Denniston, C., Orlandini, E., & Yeomans, J. M. (2001). *Phys. Rev. E*, *63*, 056702.
[24] Denniston, C., Marenduzzo, D., Orlandini, E., & Yeomans, J. M. (2004). *Phil. Trans. R. Soc. Lond. A*, *362*, 1745.
[25] Marenduzzo, D., Orlandini, E., & Yeomans, J. M. (2004). *Phys. Rev. Lett*., *92*, 188301.
[26] Marenduzzo, D., Orlandini, E., & Yeomans, J. M. (2006). *J. Chem. Phys*., *124*, 204906.
[27] Marenduzzo, D., Dupuis, A., Yeomans, J. M., & Orlandini, E. (2005). *Mol. Cryst. Liq. Cryst*., *435*, 845.
[28] Dupuis, A., Marenduzzo, D., & Yeomans, J. M. (2005). *Phys. Rev. E*, *71*, 011703.
[29] Dupuis, A., Marenduzzo, D., Orlandini, E., & Yeomans, J. M. (2005). *Phys. Rev. Lett*., *95*, 097801.
[30] Wright, D. C. & Mermin, N. D. (1989). *Rev. Mod. Phys*., *61*, 385.
[31] Shalaginov, A. N., Hazelwood, L. D., & Sluckin, T. J. (1999). *Phys. Rev. E*, *60*, 4199.
[32] Beris, A. N. & Edwards, B. J. (1994). *Thermodynamics of Flowing Systems*, Oxford University Press: Oxford.
[33] Olmsted, P. D. & Lu, C. Y. D. (1999). *Phys. Rev. E*, *60*, 4397.
[34] Marenduzzo, D., Orlandini, E., & Yeomans, J. M. (2004). *J. Chem. Phys*., *121*, 582.
[35] Orlandini, E., Marenduzzo, D., & Yeomans, J. M. (2005). *Comp. Phys. Comm*., *169*, 122.